THE JOURNAL OF BIOLOGICAL CHEMISTRY VOL. 286, NO. 19, pp. 17227–17238, May 13, 2011

Cholesteryl Ester Transfer Protein Expression Partially Attenuates the Adverse Effects of SR-BI Receptor Deficiency on Cholesterol Metabolism and Atherosclerosis*[S]

Received for publication, January 11, 2011, and in revised form, March 11, 2011 Published, JBC Papers in Press, March 20, 2011, DOI 10.1074/jbc.M111.220483

Majda El Bouhassani[‡§1], Sophie Gilibert[‡§], Martine Moreau[‡§], Flora Saint-Charles[‡§], Morgan Tréguier[‡§], Francesco Poti[‡§], M. John Chapman[‡§], Wilfried Le Goff[‡§], Philippe Lesnik[‡§], and Thierry Huby[‡§¶2]

From the [‡]INSERM UMR-S 939, Hôpital de la Pitié, F-75013, Paris, the [§]University Pierre and Marie Curie, UMR-S 939, F-75013, Paris, and the [¶]Assistance Publique-Hôpitaux de Paris, Groupe Hospitalier Pitié-Salpêtrière, Service d'Endocrinologie-Métabolisme, F-75013 Paris, France

Scavenger receptor SR-BI significantly contributes to HDL cholesterol metabolism and atherogenesis in mice. However, the role of SR-BI may not be as pronounced in humans due to cholesteryl ester transfer protein (CETP) activity. To address the impact of CETP expression on the adverse effects associated with SR-BI deficiency, we cross-bred our SR-BI conditional knock-out mouse model with CETP transgenic mice. CETP almost completely restored the abnormal HDL-C distribution in SR-BI-deficient mice. However, it did not normalize the elevated plasma free to total cholesterol ratio characteristic of hepatic SR-BI deficiency. Red blood cell and platelet count abnormalities observed in mice liver deficient for SR-BI were partially restored by CETP, but the elevated erythrocyte cholesterol to phopholipid ratio remained unchanged. Complete deletion of SR-BI was associated with diminished adrenal cholesterol stores, whereas hepatic SR-BI deficiency resulted in a significant increase in adrenal gland cholesterol content. In both mouse models, CETP had no impact on adrenal cholesterol metabolism. In diet-induced atherosclerosis studies, hepatic SR-BI deficiency accelerated aortic lipid lesion formation in both CETP-expressing (4-fold) and non-CETP-expressing (8-fold) mice when compared with controls. Impaired macrophage to feces reverse cholesterol transport in mice deficient for SR-BI in liver, which was not corrected by CETP, most likely contributed by such an increase in atherosclerosis susceptibility. Finally, comparison of the atherosclerosis burden in SR-BI liver-deficient and fully deficient mice demonstrated that SR-BI exerted an atheroprotective activity in extra-hepatic tissues whether CETP was present or not. These findings support the contention that the SR-BI pathway contributes in unique ways to cholesterol metabolism and atherosclerosis susceptibility even in the presence of CETP.

Epidemiological studies have demonstrated that high density lipoprotein cholesterol is a strong, independent, inverse predictor of the risk of coronary heart disease. High plasma levels of the major apolipoprotein of HDL, APOA-I, have been also shown to predict decreased risk of coronary heart disease. One major atheroprotective mechanism by which HDL/APOA-I may protect against atherosclerosis involves the transport of excess cholesterol from peripheral tissues, including macrophages, to the liver, bile, and eventually feces for excretion, a process known as reverse cholesterol transport.

The scavenger receptor SR-BI is an 82-kDa glycosylated plasma membrane protein that binds HDL/APOA-I with high affinity and stimulates the bi-directional flux of cholesterol between cells and extracellular HDL particles. In mice, SR-BI, encodeed by the *Scarb1* gene, is a major determinant of HDL metabolism in mice and is protective against atherosclerosis. Indeed, hepatic overexpression of SR-BI markedly reduces plasma HDL-C levels, increases biliary secretion of cholesterol, and decreases atherosclerosis (1–3), whereas deficiency of this receptor results in elevation of plasma HDL-C with the appearance of large cholesterol rich-HDL particles and is extremely pro-atherogenic (4–7). SR-BI is an important positive regulator of the rate of *in vivo* reverse cholesterol transport (RCT)[3] in mice (8). Indeed, SR-BI has the capacity to mediate the selective cellular uptake of HDL-associated cholesteryl esters in liver (9), thus facilitating a critical step of RCT. SR-BI-mediated HDL-CE selective uptake activity is also important in adrenal glands where it serves to provide cholesterol for steroid hormone synthesis in mice (9). Although SR-BI promotes cellular cholesterol efflux to HDL and LDL acceptors *in vitro*, *in vivo* RCT studies using SR-BI KO macrophages did not support a role of SR-BI, at least in mice, in the initial step of RCT (10).

One important limitation of these studies in extrapolating the importance of SR-BI from murine models to human (patho)-physiology is that mice, in contrast to humans, lack the CE transfer protein (CETP). This 74-kDa hydrophobic plasma glycoprotein transfers CE from HDL to APOB-containing lipoproteins in exchange for triglyceride and therefore exerts a key role in HDL-C metabolism. Moreover, studies in mice suggest

* This work was supported in part by the French National Institute for Health and Medical Research (INSERM).

[S] The on-line version of this article (available at http://www.jbc.org) contains supplemental Figs. S1–S3.

[1] Supported by a Fellowship from the French Ministry of Research.

[2] Supported by a contrat d'interface INSERM-APHP. To whom correspondence should be addressed: INSERM UMR-S 939, Hôpital de la Pitié, Pavillon Benjamin Delessert, 83 Boulevard de l'hôpital, F-75013 Paris, France. Tel.: 33-1-42177860; Fax: 33-1-45828198; E-mail: thierry.huby@upmc.fr.

[3] The abbreviations used are: RCT, reverse cholesterol transport; CETP, cholesteryl ester transfer protein; BMDM, bone marrow-derived macrophage; CE, cholesteryl ester; TC, total cholesterol; FC, free cholesterol.

that CETP expression may increase direct removal of HDL-CE in the liver independently of known lipoprotein receptors (11, 12). Thus, CETP, directly through hepatic selective CE uptake or indirectly through transfer of HDL-CE to APOB-containing lipoproteins with subsequent receptor-mediated liver uptake, could contribute significantly to the RCT pathway in humans. A kinetic study in humans notably suggested that most of the CE output to liver occurred through APOB-containing lipoproteins, with very little from HDL (13). These data, which favor a role of CETP in promoting RCT, are supported by studies performed in mice overexpressing CETP by adenoviral- or adeno-associated virus-mediated gene transfer (14, 15). However, a lack of effect of CETP in modulating RCT in CETP-expressing mice has also been reported and is in contradiction with the latter findings (16–18). In addition, pharmacological inhibition of CETP in humans did not significantly influence fecal sterol excretion (19).

In the present study, we have investigated whether the importance of SR-BI in controlling HDL-C metabolism as previously demonstrated in the mouse, and its overall impact on atherosclerosis, could also be evidenced in the presence of the CETP pathway. Transgenic mice expressing the human CETP gene were bred with our SR-BI conditional KO mouse (4). Our results demonstrate that the quantitative role of SR-BI in regulating the plasma levels of HDL-C was greatly diminished in the presence of CETP. Indeed, HDL metabolic studies clearly revealed that CETP expression markedly accelerated HDL-derived [^{3}H]cholesterol removal from plasma in both SR-BI liver-deficient and fully deficient mice, resulting in a significant increase of ^{3}H-labeled tracer secretion into bile and feces. However, our data also showed that whether CETP was present or not 1) SR-BI activity tightly regulates plasma free to total cholesterol (FC:TC) ratio; elevation of this ratio following liver SR-BI deficiency leading to metabolic disturbances; 2) adrenal SR-BI is critical for adrenal cholesterol content and function; and 3) hepatic SR-BI deficiency results in impaired macrophage to feces RCT. Finally, anti-atherogenic activities mediated by SR-BI in both liver and peripheral tissues could be clearly evidenced under non- and CETP-expressing conditions. Altogether, these data suggest that the SR-BI pathway may be of critical importance in cholesterol homeostasis and, potentially in atherosclerosis, in humans.

EXPERIMENTAL PROCEDURES

Animal Models and Diet—The investigation conformed to the Guide for the Care and Use of Laboratory Animals published by the European Commission Directive 86/609/EEC. All animal procedures were performed at the Central Animal Facility of the Medical Faculty of La Pitié Hospital with approval from the Direction Départementale des Services Vétérinaires, Paris, France. Mice were housed in a conventional animal facility, weaned at 21 days, and fed *ad libitum* a normal mouse chow diet (RM1, Dietex France). All animal models were bred on a pure C57BL/6 background (>10 generations). The SR-BI conditional knock-out mouse model, in which *Scarb1* exon 1 targeted by the CRE recombinase loxP site insertion produced a hypomorphic allele, has been described earlier (4) and was termed the hypomSR-BI mouse. CRE-mediated *Scarb1* gene inactivation of the hypomorphic SR-BI allele in hepatocytes (hypomSR-BI KO^{liver} mice) was obtained through breeding with Alb-CRE transgenic mice (20). SR-BI$^{-/-}$ mice were described previously (4) and generated by breeding homozygous animals fed a chow diet containing 0.5% probucol (Sigma). Human CETP transgenic mice, which express CETP under control of its natural flanking regions (NFR-CETP line 5203), were obtained from Jackson Laboratories (Bar Harbor, MC). For atherosclerosis studies, 2-month-old female mice were switched to a 1.25C diet, consisting of 1.25% cholesterol and 20% fat for 20 weeks (standard A04 diet supplemented with 1.25% cholesterol and 16% cocoa butter; SAFE, Augy, France).

Blood and Tissue Analyses—Blood samples were collected in Microvette tubes (Sarstedt) by retro-orbital bleeding under isoflurane anesthesia (isoflurane (1.5%), oxygen (0.4 liter/min)). Plasma samples were analyzed with an Autoanalyzer using commercial reagent kits (Roche Diagnostics (total cholesterol), Diasys (free cholesterol), and ThermoElectron (glucose)). Plasma lipoproteins were fractionated by gel filtration on two Superose 6 (Amersham Biosciences) columns connected in series. Endogenous plasma lecithin:cholesterol acyltransferase activity was determined by measuring the decrease in plasma-free cholesterol following incubation at 37 °C in the presence or absence of iodoacetamide (lecithin:cholesterol acyltransferase inhibitor). To determine cholesterol and phospholipids content of red blood cells (RBC), packed RBC were mixed with an equal volume of water to achieve hemolysis. To extract lipids from RBC, a mixture of hexane:isopropyl alcohol, 3:2, was added and samples were mixed. After centrifugation, supernatants were collected, evaporated, and resuspended in isopropyl alcohol. Lipids were measured by enzymatic colorimetric methods. Plasma corticosterone levels were determined by a commercial competitive enzyme immunoassay kit (Immunodiagnostic Systems). To determine cholesterol content in adrenal glands, total lipids were extracted from frozen organs using the Folch procedure.

Erythrocyte, Reticulocyte, and Platelet Counts—Absolute count of erythrocytes, reticulocytes, and platelets were performed by flow cytometry (BD LSR Fortessa, BD Biosciences). Whole blood (1 μl) was incubated with either 1 μl of phycoerythrine anti-mouse CD41 (clone MWReg30, eBiosciences) for determination of platelets or 1 μl of each phycoerythrine anti-mouse Ter-119 (clone Ter-119, Miltenyi Biotec) and allophycocyanin anti-mouse CD71 (clone R17 217.1.4, eBiosciences) for determination of erythrocytes and reticulocytes, respectively. After 15 min at room temperature, samples diluted in 0.5 ml of PBS, 0.5% BSA, 2 mM EDTA, and 0.1 ml of counting beads, with an established concentration close to 1000 beads/μl^{-1} (FlowCount Fluorospheres, Beckman Coulter), were added to express population counts as absolute number per microliter of whole blood.

Analysis of Atherosclerotic Plaques—Atherosclerotic lesions were quantified on serial cross-sections (10 μm) through the aortic root by oil red O staining as previously described (21), with minor modifications. Mice were sacrificed under isoflurane anesthesia and perfused with PBS. Hearts were collected and fixed (Accustain, 10% formalin solution (Sigma) supplemented with 2 mM EDTA and 20 μM butylated hydroxytoluene

at pH 7.4) for 30 min followed by overnight incubation in phosphate-buffered 20% sucrose solution at 4 °C; hearts were subsequently embedded in Tissue-Tek OCT compound (Sakura Finetek). Approximately 40 sections, 10-μm thick, were cut through the proximal aorta, spanning the three cusps of the aortic valves. Every eighth section was fixed and stained with oil red O (0.3% in triethylphosphate) for 30 min and then counterstained with Mayer hematoxylin for 1 min. Images were captured using a Zeiss Axiovert 135 microscope and analyzed with Adobe Photoshop 7.0 software (Adobe Systems Inc., CA) and the Image Processing Tool Kit (Reindeer Graphics, NC) plugins. The extent of atherosclerosis was measured with color thresholding to delimit areas of oil red O staining and is reported as mean lesion area of the group of the sections analyzed.

In Vivo HDL Turnover Studies—Mouse plasma was incubated with [^{3}H]cholesterol (4 μCi/ml) for 16 h at 37 °C. [^{3}H]Cholesterol-labeled mouse HDL were then isolated from plasma by sequential ultracentrifugation in the density range of $1.063 < d < 1.21$ g/ml, dialyzed against PBS and filter-sterilized. Labeled HDL (80 μg of HDL protein, 0.4×10^6 cpm) were injected in a volume of 200 μl by retro-orbital injection in the right eye of the anesthetized mouse. Mice were caged separately on a wire mesh with unlimited access to food and water. Blood samples were collected by retroorbital bleeding (75 μl) in the left eye at 3 min, 2 h, and 6 h after injection. 24 h after injection, mice were exsanguinated under isoflurane anesthesia and sacrificed by cervical dislocation. Bile was collected by direct puncture of the gall bladder with a syringe (30-gauge needle) during the initial stage of laparotomy. Mice were then perfused extensively with PBS before harvesting their organs (liver, adrenal glands, kidney, spleen, leg muscle, gonadal white adipose tissue). Bone marrow cells were flushed with PBS from femurs, and cells were depleted of erythrocytes by ACK treatment for 5 min before cell counting. Collected blood was centrifuged and plasma was collected. ^{3}H radioactivity in plasma was determined by liquid scintillation counting and plasma decay curves for ^{3}H-labeled tracer were normalized to radioactivity at the initial 3-min time point. Lipids in red blood cells were extracted as described above and [^{3}H]cholesterol was counted in the lipid extract. Values were normalized to radioactivity present in plasma at the initial 3-min time point. Collected tissues and feces were treated as described above and counted in a liquid scintillation counter.

In Vivo Macrophage to Feces RCT Assay—Macrophage to feces RCT was evaluated *in vivo* using the assay developed by Zhang and colleagues (22), which measures transport of cholesterol from intraperitoneally injected [^{3}H]cholesterol-labeled macrophages to plasma, liver, adrenals, and feces. Injected macrophages were derived from bone marrow cells (BMDM) isolated from wild-type C57BL/6 mice. BMDM were flushed with PBS from femurs of freshly euthanized mice. Cells were depleted of erythrocytes by ACK treatment for 5 min and plated for 5 days in DMEM supplemented with penicillin/streptomycin antibiotics, 1 mM glutamine, 10% heat inactivated FBS, and 30% L929 conditioned medium as a source of macrophage colony stimulating factor. BMDM were then cholesterol loaded by adding complete medium supplemented with 50 μg/ml of acetylated LDL protein labeled with 5 μCi of [^{3}H]cholesterol/ml, and cultured for two additional days. Cholesterol-loaded and [^{3}H]cholesterol-labeled BMDM were detached from plastic by accutase (PAA) treatment, washed, resuspended in PBS at room temperature, and injected (0.5 ml; 5×10^6 cells) intraperitoneally. Mice were caged separately on a wire mesh, with unlimited access to food and water, and stools were collected continuously over the next 2 days. At 48 h post-injection, mice were exsanguinated by retro-orbital bleeding under isoflurane anesthesia, sacrificed by cervical dislocation, and then perfused extensively with PBS. Whole livers and adrenal glands were collected, weighed, and flash frozen. ^{3}H-Labeled radioactivity in plasma was determined by liquid scintillation counting and expressed as counts/min/μl of plasma. Pooled plasmas from each group were also fractionated by gel filtration to determine cholesterol mass and ^{3}H-labeled tracer distribution into lipoproteins. For each mouse, total feces were dried, weighed, soaked in water (1 ml of water/57 mg of desiccated feces; overnight at 4 °C) and mechanically homogenized. Homogenized samples (0.2 ml) were added to 10 ml of liquid scintillation OptiPhase HiSafe 3 (PerkinElmer Life Sciences) mixture and counted in a liquid scintillation counter (Beckman LS 6000IC). ^{3}H-Labeled counts in liver and adrenal glands were determined after homogenization of the tissue in water (~100 mg piece of liver tissue/ml; one adrenal gland/0.4 ml) and counting was performed in a liquid scintillation counter (0.3 and 0.4 ml of homogenized samples combined with 10 ml of OptiPhase HiSafe 3 mixture). For the RCT studies performed with ezetimibe-treated mice, the animals were first accustomed to powdered chow diet (RM1, Dietex France) for 2 weeks, and then switched to the same powdered diet supplemented with 0.005% ezetimibe (Schering-Plough) for 9 days before starting the RCT assay. During the experiment, individually housed mice were also fed the ezetimibe-supplemented diet.

Statistical Analysis—One-way analysis of variance and Tukey's post hoc multiple comparison tests were used to assess statistical significance between groups. All statistical analyses were performed using GraphPad Prism software (GraphPad Software, Inc., San Diego, CA). $p < 0.05$ was considered significant.

RESULTS

Impact of CETP Expression on Plasma Cholesterol Levels and Hematologic Parameters of SR-BI-deficient Mice—CETP expression diminishes plasma total cholesterol levels and has a major impact on HDL cholesterol content and particle size in SR-BI$^{-/-}$ mice (23, 24). Under chow diet feeding, we also observed that SR-BI$^{-/-}$/CETP mice exhibited a 1.5-fold decrease in plasma TC as compared with non-CETP transgenic animals (Table 1). Decreased plasma TC levels were also observed following CETP expression in mice with either attenuated SR-BI expression (hypomSR-BI) or in mice with CRE-mediated deletion of hepatic SR-BI (hypomSR-BI KO^{liver}). Under high cholesterol feeding (1.25C diet), CETP expression also significantly reduced plasma TC in all SR-BI models with the exception of WT animals (Table 2). Analysis of lipoproteins by size exclusion chromatography (Fig. 1, *A* and *C*) or by agarose gel electrophoresis (Fig. 1, *B* and *D*) revealed that CETP

TABLE 1

Plasma cholesterol levels, lecithin:cholesterol acyltransferase (LCAT) activity, hematocrit, and spleen weight of mice fed a chow diet

Values were determined in overnight fasted age-matched mice fed a chow diet. Data represent mean ± S.D. Spleen mass was expressed per g of body weight. Lecithin: cholesterol acyltransferase activity is expressed as nanomol of CE transferred/h/ml.

Genotype	Gender	TC	FC:TC	LCAT activity	Hematocrit	Spleen
		mg/dl	*%*		*%*	*mg/g*
WT	F	73 ± 9	29 ± 2		47.4 ± 1.4	3.7 ± 0.3
	M	94 ± 3	25 ± 1	257 ± 49	48.4 ± 1.1	3.1 ± 0.5
WT/CETP	F	68 ± 13	28 ± 2		47.0 ± 2.9	4.2 ± 0.6
	M	83 ± 6	25 ± 1	224 ± 5	47.9 ± 0.9	3.0 ± 0.7
HypomSR-BI	F	130 ± 12[a]	30 ± 1		47.6 ± 1.7	3.7 ± 0.3
	M	156 ± 10[a]	31 ± 1[b]	177 ± 51	46.9 ± 2.1	3.1 ± 0.8
HypomSR-BI/CETP	F	100 ± 15[a,c]	31 ± 2		49.0 ± 2.6	3.9 ± 0.6
	M	111 ± 14[c]	33 ± 2[a]	233 ± 76	47.5 ± 2.2	3.1 ± 0.4
HypomSR-BI KO^{liver}	F	176 ± 13[a]	49 ± 5[a]		45.5 ± 1.9	5.9 ± 0.7[a]
	M	182 ± 10[a]	51 ± 3[a]	112 ± 30[a]	44.7 ± 2.2[b]	5.4 ± 1.5[a]
HypomSR-BI KO^{liver}/CETP	F	110 ± 9[a,c]	49 ± 5[a]		46.8 ± 1.6	4.7 ± 0.4[b,d]
	M	117 ± 24[b,c]	49 ± 4[a]	230 ± 59[d]	45.1 ± 2.1[b]	3.8 ± 0.6[c]
SR-BI$^{-/-}$	F	147 ± 6[a]	51 ± 3[a]		43.1 ± 1.6[b]	6.6 ± 0.6[a]
	M	137 ± 14[a]	52 ± 6[a]	106 ± 50[b]	42.3 ± 1.9[a]	5.9 ± 1.6[a]
SR-BI$^{-/-}$/CETP	F	107 ± 9[a,c]	47 ± 3[a]		43.5 ± 1.9[b]	6.2 ± 0.7[a]
	M	94 ± 10[c]	48 ± 1[a]	265 ± 72[d]	42.1 ± 1.6[a]	4.5 ± 0.8[b,d]

[a] $p < 0.001$, statistically different from values for control mice.
[b] $p < 0.05$, statistically different from values for control mice.
[c] $p < 0.001$, statistically different from values for corresponding non-CETP transgenic mice.
[d] $p < 0.05$, statistically different from values for corresponding non-CETP transgenic mice.

TABLE 2

Plasma lipid levels, hematocrit, and spleen weight of mice fed an atherogenic diet

Values were determined in overnight fasted female mice fed a 1.25% cholesterol diet for 20 weeks. Data represent mean ± S.D. Spleen mass was expressed per g of body weight.

Genotype	TC	FC:TC	Hematocrit	Spleen
	mg/dl		*%*	*mg/g*
WT	85 ± 17	26 ± 6	44.3 ± 3.2	4.3 ± 1.3
WT/CETP	101 ± 23	24 ± 6	44.8 ± 1.7	4.6 ± 1.1
HypomSR-BI	180 ± 20[a]	27 ± 2	45.8 ± 2.9	3.8 ± 1.0
HypomSR-BI/CETP	158 ± 15[a]	27 ± 2	42.9 ± 3.8	4.6 ± 0.9
HypomSR-BI KO^{liver}	331 ± 56[a]	62 ± 3[a]	35.9 ± 6.2[a]	22.0 ± 5.9[a]
HypomSR-BI KO^{liver}/CETP	227 ± 48[a,b]	61 ± 6[a]	34.4 ± 3.9[a]	21.3 ± 7.6[a]
SR-BI$^{-/-}$	311 ± 43[a]	62 ± 3[a]	34.3 ± 3.9[a]	25.8 ± 6.7[a]
SR-BI$^{-/-}$/CETP	249 ± 28[a,c]	62 ± 3[a]	35.0 ± 4.1[a]	22.2 ± 5.0[a]

[a] $p < 0.001$, statistically different from values for control mice.
[b] $p < 0.001$, statistically different from values for corresponding non-CETP transgenic mice.
[c] $p < 0.05$, statistically different from values for corresponding non-CETP transgenic mice.

expression resulted in the disappearance of the large cholesterol-rich HDL particles generated by reduced/deficient hepatic SR-BI expression, thereby demonstrating the capacity of CETP to unload CE from HDL independently of the hepatic SR-BI receptor (Fig. 1). SR-BI deficiency (7, 25), and more precisely hepatic SR-BI deficiency (4), results in a specific accumulation of free cholesterol in plasma, which translates into a >1.5-fold increase in the FC:TC ratio in hypomSR-BI KO^{liver} and SR-BI$^{-/-}$ mice as compared with controls (Table 1). Reduced endogenous plasma lecithin:cholesterol acyltransferase activity in both SR-BI fully and liver-deficient mouse models (Table 1) corroborated earlier findings of a significant inhibition of the endogenous cholesterol esterification rate in plasma of SR-BI$^{-/-}$ mice (26, 27). Interestingly, whereas CETP expression restored plasma lecithin:cholesterol acyltransferase activity to normal in both hypomSR-BI KO^{liver} and SR-BI$^{-/-}$ mice, it did not change the FC:TC ratio, which remained elevated (Table 1). This observation very strongly reinforces the notion that hepatic SR-BI is a major determinant of plasma FC levels and is in agreement with earlier findings demonstrating a critical role of SR-BI in the clearance of HDL-FC from plasma (28).

It has been previously reported that SR-BI deficiency is associated with mild anemia (29), which is exacerbated by feeding mice a high cholesterol diet (30). Hematocrits were indeed significantly lower in SR-BI$^{-/-}$ mice but also in hypomSR-BI KO^{liver} mice (Table 1). Upon feeding a 1.25C diet, this anemia was exacerbated in both models (Table 2). Meurs and colleagues (29) have suggested that erythrocyte cholesterol enrichment, as a result of increased plasma FC levels in SR-BI$^{-/-}$ mice, reduces the lifespan of erythrocytes and consequently enhances erythropoiesis, which in turn favors reticulocytosis and splenomegaly in these animals. In the present study, circulating erythrocytes in SR-BI$^{-/-}$ mice were decreased 1.7-fold as compared with WT controls (Fig. 2*A*), whereas the amount of immature erythrocytes (reticulocytes) was significantly increased to reach 6.9 ± 1% of the erythrocyte population (as compared with 2.5 ± 0.1% in WT) (Fig. 2*B*). Invalidation of SR-BI in liver resulted in a similar phenotype, with a 1.8-fold decrease in erythrocyte counts associated with a 3.6-fold elevation in the amount of reticulocytes. CETP had no major impact on the decreased hematocrit of both hypomSR-BI KO^{liver} and SR-BI-deficient mice (Tables 1 and 2). However, its expression attenuated erythrocyte abnormalities in both models (Fig. 2, *A* and *B*). The splenomegaly present in SR-BI-deficient animals was also less pronounced when they expressed CETP in chow fed (Table 1), but not in high cholesterol fed conditions (Table 2). Thus, it appears that the increased plasma FC levels resulting from SR-BI deficiency cannot solely explain alteration in RBC metabolism. Indeed, CETP expression had no impact on the elevated plasma FC:TC ratio in these mice but partially restored RBC defects. Hypercholesterolemia must also contribute to the altered RBC metabolism in SR-BI-deficient mice. The high plasma FC:TC ratio in SR-BI$^{-/-}$ mice has also been correlated with thrombocytopenia (31). If fully deficient and liver-deficient mice for SR-BI similarly displayed diminished platelet counts (~2-fold), CETP expression in the latter model partially restored platelet counts, whereas no significant effect was seen in SR-BI$^{-/-}$ mice (Fig. 2*C*). These results suggest that platelet

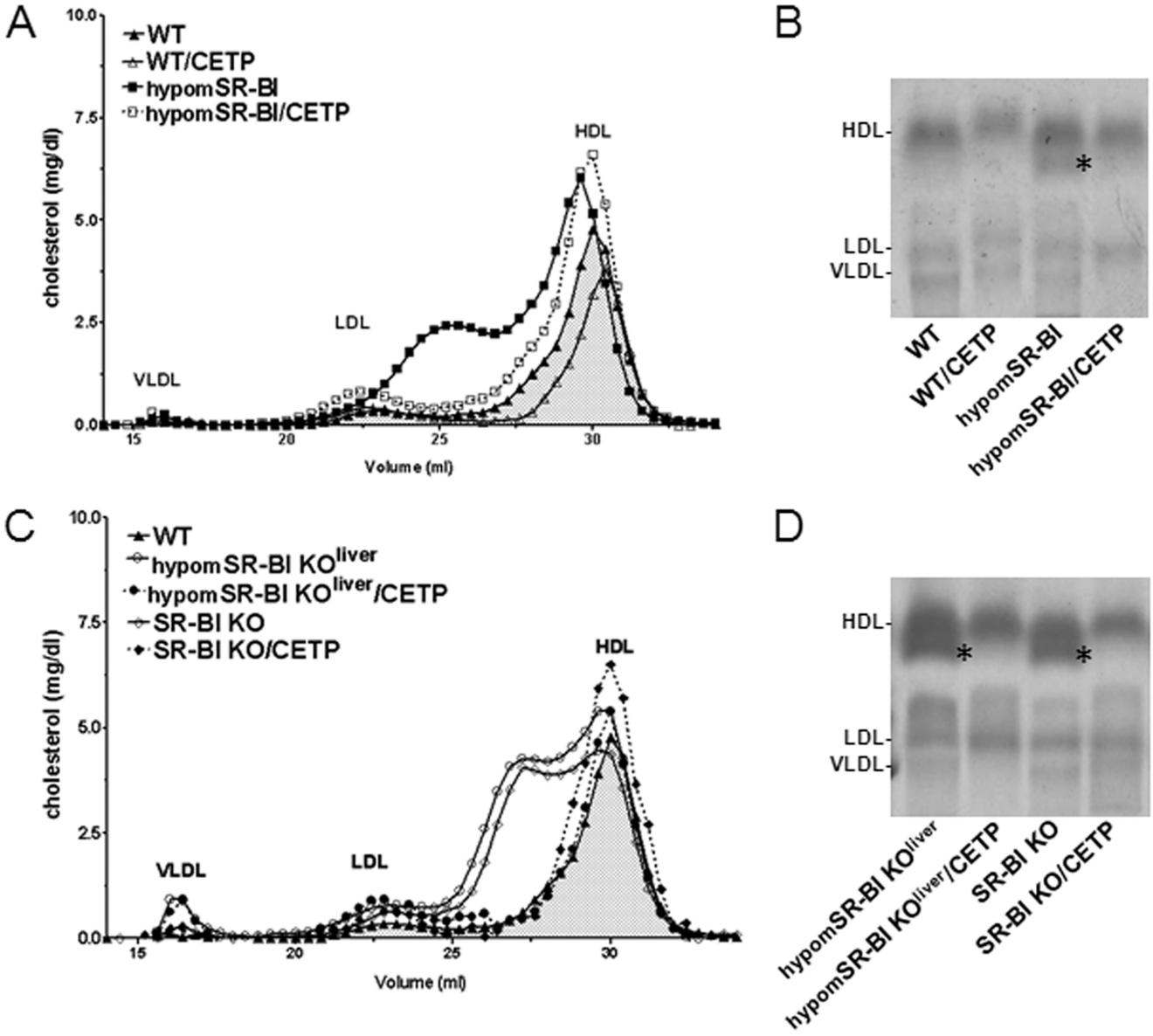

FIGURE 1. **Impact of CETP and SR-BI expression on plasma lipoprotein cholesterol profiles of SR-BI-deficient mice.** *A* and *C*, fasting plasma samples from 2-month-old male mice fed a chow diet were fractionated by size exclusion chromatography. Total cholesterol was measured in each fraction to determine lipoprotein cholesterol profiles. Approximate elution volumes for particles in the size ranges of VLDL, LDL, and HDL are indicated. *B* and *D*, electrophoretic mobilities of plasma lipoproteins analyzed on agarose gels. Lipoproteins were revealed by Sudan black staining. * indicates the presence of larger HDL exhibiting a lower electronegativity.

SR-BI deficiency could contribute to thrombocytopenia in SR-BI$^{-/-}$/CETP animals. Finally, it is noteworthy that hypomSR-BI mice (expressing CETP or not) displayed normal erythrocyte, reticulocyte, and platelet counts (Fig. 2) and did not possess enlarged spleens (Tables 1 and 2) as opposed to hypomSR-BI KO^{liver} mice. These results further link hepatic SR-BI deficiency to the altered free cholesterol metabolism and as a consequence hematologic disturbances.

CETP Expression Does Not Modulate Cholesterol Homeostasis in Adrenal Glands nor Adrenal Corticosterone Production—SR-BI is considered to be primarily responsible for the selective uptake of HDL-CE by the adrenals in mice (9). As a consequence and as previously reported (6), the cholesterol content of adrenal glands of SR-BI$^{-/-}$ mice is markedly reduced (5-fold, $p < 0.001$; Fig. 3*A*). Staining adrenal tissue for neutral lipids clearly confirmed the presence of significantly less lipid accumulation in the adrenal cortex of these mice (Fig. 3*B*). Adrenal glands of SR-BI$^{-/-}$ mice were equally significantly enlarged (Table 3). Knock-down expression of SR-BI in hypomSR-BI mice was also associated with decreased adrenal cholesterol storage (66% of controls, $p < 0.05$; Fig. 3*A*), but to a lower extent than that seen in SR-BI$^{-/-}$ mice; significantly the adrenals of these animals were of normal size (Table 3). Remarkably, analysis of the adrenal glands of hypomSR-BI KO^{liver} mice revealed a 1.3-fold increase in cholesterol content as compared with controls ($p < 0.05$; Fig. 2*A*) and intense lipid staining of the cortex (Fig. 3*B*), despite similar adrenal SR-BI expression in this line as compared with those measured in hypomSR-BI mice (Fig. 3*C*). Hoekstra and co-workers (32) demonstrated that adrenal glucocorticoid-mediated stress response to fasting was

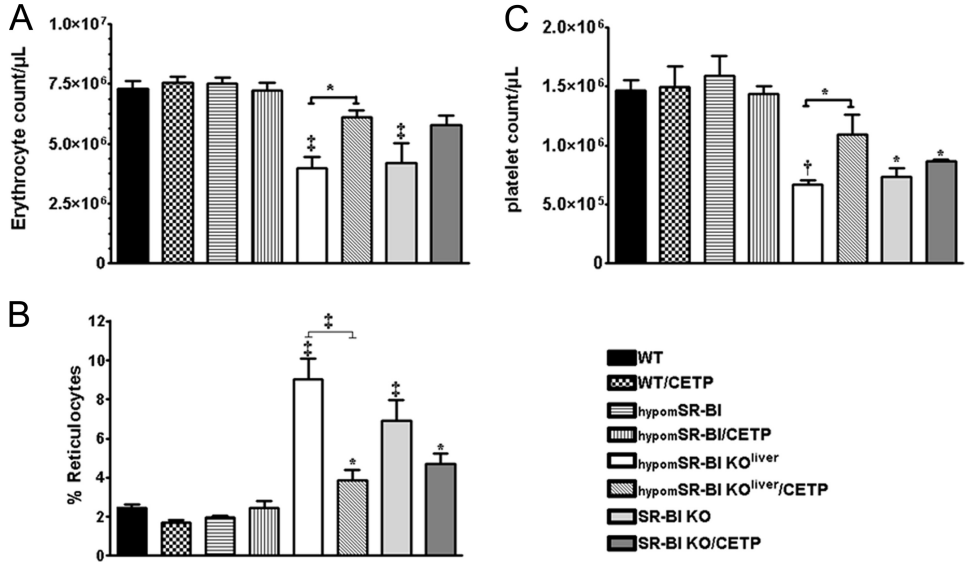

FIGURE 2. **Erythrocyte, reticulocyte, and platelet counts.** Blood isolated from male mice was analyzed by flow cytometry to determine the absolute counts of erythrocytes (*A*), reticulocytes (expressed as a percentage of total erythrocytes) (*B*), and platelets (*C*) ($n = 4$–9; data represent mean ± S.E.). *, †, and ‡ denote a statistical difference *versus* WT mice or between indicated groups, *, $p < 0.05$; †, $p < 0.01$; and ‡, $p < 0.001$.

impaired in SR-BI$^{-/-}$ mice due to adrenal glucocorticoid insufficiency, which led to hypoglycemia. We found similar results, plasma corticosterone and glucose levels being 1.9- and 1.5-fold lower in fasted SR-BI$^{-/-}$ female mice than in fasted WT controls, respectively (Table 3). CETP expression had no impact on cholesterol stores and weight of the adrenals of any of the mouse models studied nor did it influence plasma corticosterone and glucose levels following overnight fasting (Fig. 3 and Table 3).

To determine whether changes in adrenal cholesterol content were associated with changes in the expression of genes involved in cellular cholesterol homeostasis, we performed real time PCR quantification. The gene expression profile was consistent with a normal adaptive response of adrenal cortical cells to variation in their intracellular cholesterol status via SREBP2-mediated transcriptional gene regulation to either reduce (hypomSR-BI KO^{liver}) or increase (hypomSR-BI, SR-BI$^{-/-}$) cholesterol uptake through the LDL-r pathway and cholesterol biosynthesis and, via L*X*R-mediated regulation to limit (hypomSR-BI, SR-BI$^{-/-}$) or enhance (hypomSR-BI KO^{liver}) cellular cholesterol efflux (Fig. 3*C*). The lack of effect of CETP expression on adrenal cholesterol stores was confirmed at the mRNA level because expression levels of cholesterol-responsive genes in adrenals of WT, hypomSR-BI, hypomSR-BI KO^{liver}, or SR-BI$^{-/-}$ mice were similar whether these mouse models expressed CETP or not (Fig. 3*C*).

CETP Expression Fails to Restore Impaired Macrophage to Feces RCT in SR-BI-deficient Mice—CETP reduces plasma HDL-C levels in SR-BI-deficient mice, potentially providing an alternative pathway to RCT. We therefore evaluated the impact of CETP on the metabolic fate of mouse HDL-derived cholesterol in SR-BI liver-deficient and fully deficient female mice fed a 1.25C diet for 4 weeks. As previously reported (9), [^{3}H]cholesterol-HDL was cleared more slowly from plasma in SR-BI-deficient mice than in WT animals (Fig. 4*A*). CETP expression in SR-BI$^{-/-}$ mice accelerated clearance of the ^{3}H-labeled tracer from plasma to an even faster rate than that observed in WT. 24 h after labeled HDL injection, ^{3}H-labeled tracer was found markedly reduced in liver and bile of SR-BI$^{-/-}$ mice, whereas SR-BI$^{-/-}$ mice expressing CETP displayed comparable ^{3}H-counts to WT controls (Fig. 4*B*). As expected from these results, CETP expression in SR-BI$^{-/-}$ mice resulted in a significant increase in ^{3}H-counts in feces (3.5-fold, $p < 0.001$). However, the amount of ^{3}H-labeled tracer recovered in feces of SR-BI$^{-/-}$/CETP mice was still below that found in feces of WT (1.5-fold, $p < 0.001$). If no difference in ^{3}H-counts was notable between the mouse models in kidney and spleen (also in white adipose tissue, bone marrow cells, and muscle, data not shown), SR-BI-deficient mice (±CETP) displayed a 6-fold decrease in radioactivity in their adrenals as compared with WT (Fig. 4*B*). These data are in agreement with diminished adrenal cholesterol store in SR-BI$^{-/-}$ mice (Fig. 3) and further confirm the lack of effect of CETP expression on adrenal cholesterol homeostasis in mice. In addition, we also found that the amount of ^{3}H-labeled tracer was doubled in erythrocytes of SR-BI$^{-/-}$/CETP mice, but also of SR-BI$^{-/-}$ mice, as compared with WT (Fig. 4*B*). These results are in agreement with a specific enrichment in cholesterol measured in erythrocytes of SR-BI-deficient mice expressing CETP or not (~1.4-fold elevation in the cholesterol to phospholipid ratio; supplemental Fig. S1). Finally, [^{3}H]cholesterol-HDL injection in hypomSR-BI, hypomSR-BI KO^{liver}, and hypomSR-BI KO^{liver}/CETP mice provided similar results as those found with the mice fully deficient for SR-BI (supplemental Fig. S2). Thus, these HDL metabolic studies confirmed the capacity of CETP to accelerate impaired RCT from plasma HDL in SR-BI-deficient mice (or SR-BI liver-deficient mice). This CETP-dependent effect most likely contributed to the net loss of plasma cholesterol observed in all SR-BI mouse models expressing CETP.

We next sought to evaluate whether CETP expression had the potential to stimulate the impaired macrophage to feces RCT associated with SR-BI deficiency. [^{3}H]Cholesterol-labeled

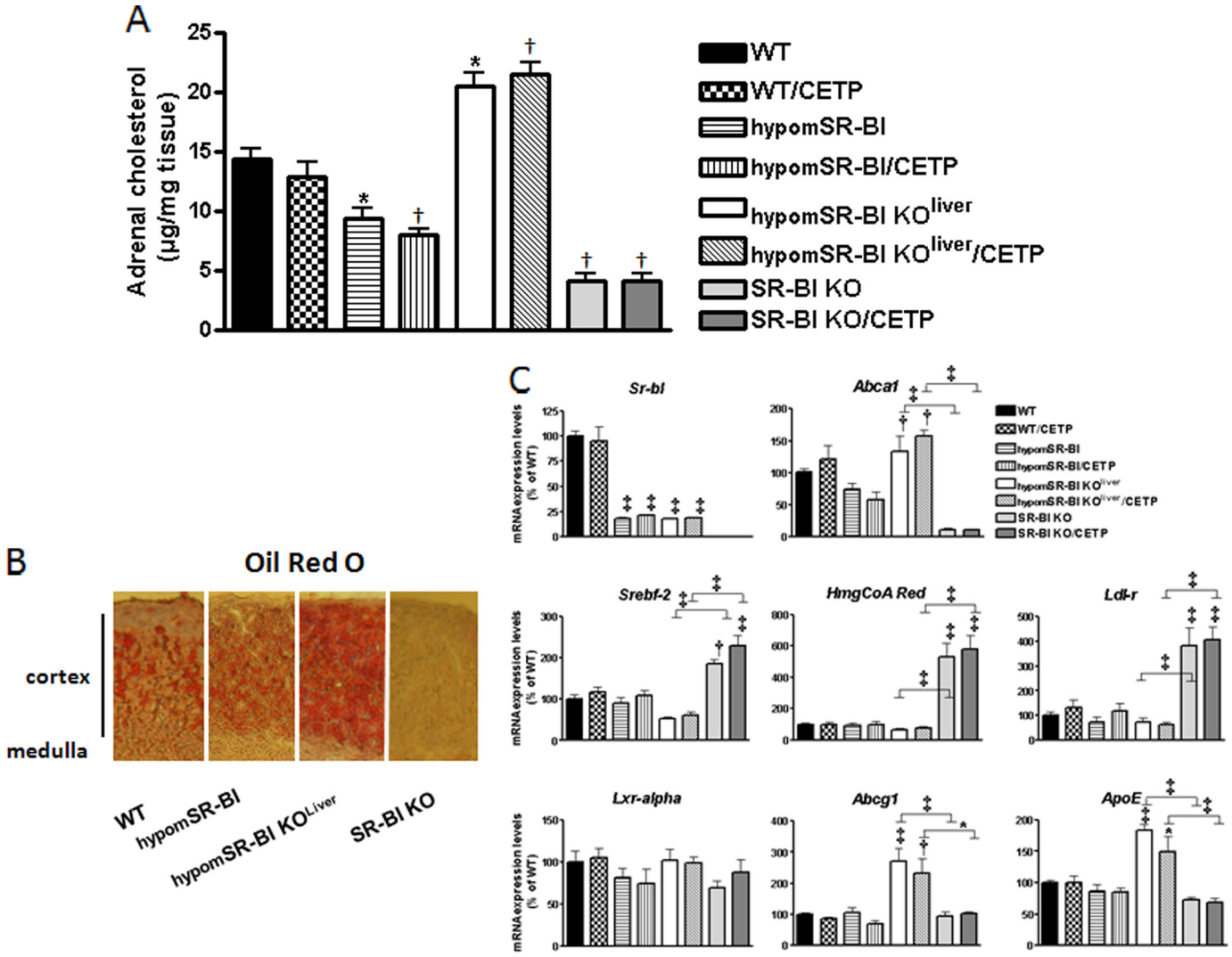

FIGURE 3. **Impact of CETP and SR-BI expression on adrenal cholesterol content and gene expression profiling.** *A*, cholesterol content of adrenal glands of fasting 3-month-old mice was determined after lipid extraction ($n = 8–18$; data represent mean ± S.E.). * and † statistically different from values for WT mice, *, $p < 0.05$; †, $p < 0.001$. Cryosections of adrenal glands were analyzed for lipids by ORO staining (*B*). Adrenal gene expression profiling of mice fed a chow diet was obtained by quantitative PCR analysis. For each gene, values were normalized to hypoxanthine-guanine phosphoribosyltransferase and plotted relative to those of wild-type mice set at 100% ($n = 5–6$; data represent mean ± S.E.). *, †, and ‡ denote a statistical difference *versus* WT mice or between indicated groups, *, $p < 0.05$; †, $p < 0.01$; ‡, $p < 0.001$.

TABLE 3

Adrenal weight and plasma corticosterone and glucose levels of fasted mice

Values were determined in overnight fasted 3-month-old female mice fed a chow diet. Data represent mean ± S.D. Adrenal mass was expressed per g of body weight.

Genotype	Adrenals	Corticosterone	Glucose
	mg/g	*ng/ml*	*mg/dl*
WT	0.12 ± 0.02	164 ± 34	126 ± 31
WT/CETP	0.13 ± 0.03	151 ± 29	130 ± 14
HypomSR-BI	0.13 ± 0.02	175 ± 56	131 ± 28
HypomSR-BI/CETP	0.13 ± 0.01	149 ± 45	131 ± 33
HypomSR-BI KO^{liver}	0.13 ± 0.01	145 ± 28	129 ± 33
HypomSR-BI KO^{liver}/CETP	0.13 ± 0.02	157 ± 19	131 ± 33
SR-BI$^{-/-}$	0.20 ± 0.03[a]	88 ± 23[b]	80 ± 16[b]
SR-BI$^{-/-}$/CETP	0.21 ± 0.03[a]	87 ± 20[b]	90 ± 13[b]

[a] $p < 0.001$, statistically different from values for WT mice.
[b] $p < 0.05$, statistically different from values for WT mice.

bone marrow-derived macrophages were injected in WT, hypomSR-BI KO^{liver}, and hypomSR-BI KO^{liver}/CETP mice. Plasma [^{3}H]cholesterol was substantially increased in hypomSR-BI KO^{liver} mice as compared with WT, but was lowered in CETP-expressing hypomSR-BI KO^{liver} mice (Fig. 5*A*); reflecting plasma cholesterol mass in these models (Fig. 1 and Table 1). The amount of ^{3}H-sterol measured per mg of liver and feces over 48 h was significantly reduced in both hypomSR-BI KO^{liver} and hypomSR-BI KO^{liver}/CETP mice as compared with controls. However, ^{3}H values were not different between these two models (Fig. 5*A*). These data are indicative of a decreased rate of macrophage to feces RCT in SR-BI liver-deficient mice, as previously reported in the animals that were fully deficient (8). However, if CETP expression significantly accelerated RCT from plasma HDL in hypomSR-BI KO^{liver} mice (supplemental Fig. S2), it had no effect on impaired macrophage to feces RCT (Fig. 5*A*). A similar result was also found in the context of a functional (WT mice) or an impaired RCT pathway due to complete SR-BI deficiency (supplemental Fig. S3*A*).

To further evaluate whether an impact of CETP on macrophage to feces RCT rate could be evidenced in SR-BI-deficient mice by increasing the flux of cholesterol in the animals, we fed

A

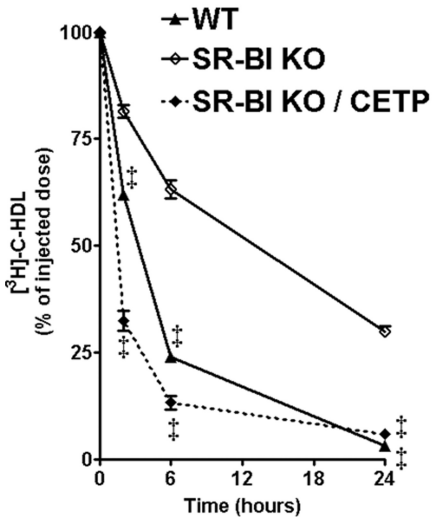

B

Genotype	WT (n=8)	SR-BI KO (n=6)	SR-BI KO / CETP (n=5)
Liver	102±4 (29±3)	38±4† (12±2)	89±4 § (30±1)
Feces	42±2 (6.0±0.9)	11±1† (1.1±0.4)	31±1†,§ (3.9±0.6)
Bile	219±13 (0.45±0.21)	61±6† (0.11±0.03)	194±19§ (0.57±0.06)
Adrenal	234±18 (0.20±0.05)	37±3† (0.07±0.01)	33±3† (0.05±0.01)
Kidney	7.6±0.5 (0.42±0.05)	8.2±0.6 (0.48±0.10)	8.6±0.4 (0.47±0.02)
Spleen	8.4±0.4 (0.17±0.03)	7.5±0.4 (0.92±0.25)	7.5±0.5 (0.62±0.09)
Red Blood cells	5.6±0.5 (2.0±0.3)	11±0.6† (4.3±0.3)	12±0.5† (4.5±0.4)

FIGURE 4. **Impact of CETP and SR-BI expression on the metabolic fate of HDL-C.** *A*, plasma decay over 24 h of [^{3}H]cholesterol-labeled mouse HDL injected in wild-type, SR-KO, and SR-BI KO/CETP female mice fed a 1.25C diet. ‡ statistically different from values for SR-BI KO mice at the indicated time point. *B*, 24 h post-injection the animals were sacrificed and the tissue distribution of radioactivity was determined. Data are expressed as cpm/mg of wet tissue or dried feces, except for bile and bone marrow cells for which values are expressed as cpm/μl and cpm/million cells, respectively. Values represent mean ± S.E. *Values in parentheses* correspond to the percentage of the injected dose present in the organ. * and †, statistically different from values for WT mice, *, $p < 0.05$; †, $p < 0.001$. ‡ and §, statistically different from values for SR-BI KO mice, ‡, $p < 0.05$; §, $p < 0.001$.

WT and SR-BI$^{-/-}$ mice expressing or not CETP a 1.25C diet for 4 weeks before performing an *in vivo* RCT assay (Fig. 5*B*). [^{3}H]Cholesterol was equilibrated in the plasma of cholesterol-fed mouse models in proportion to their cholesterol mass (Table 2). As expected, the amount of [^{3}H]cholesterol tracer detected in liver, feces, and adrenals of SR-BI$^{-/-}$ mice was statistically significantly lower (1.6-, 2.2-, and 2.6-fold, respectively) than those measured for WT. Results obtained with WT/CETP and SR-BI$^{-/-}$/CETP mice did not differ from those of WT and SR-BI$^{-/-}$ mice, respectively, further confirming a lack of effect of CETP in promoting macrophage to feces RCT in our experimental conditions.

Using similar *in vivo* RCT studies, Sehayek and Hazen (33) have recently reported that decreased cholesterol absorption through ezetimibe treatment significantly increases fecal cholesterol excretion; thereby supporting a major role of intestinal cholesterol absorption in RCT in mice. Thus, we evaluated whether treating our animal models with ezetimibe could reveal an effect of CETP on the RCT rate, which could have been masked in our previous experiments by elevation of intestinal cholesterol (re)-absorption in CETP-expressing mouse models. Ezetimibe treatment of WT animals resulted in an ~2-fold increase in fecal ^{3}H-sterol excretion as compared with non-treated WT controls (supplemental Fig. S3*B*). However, CETP expression resulted in no significant change in the amount of ^{3}H-labeled tracer measured in liver, feces, and adrenals in both ezetimibe-treated WT and SR-BI-deficient mouse models.

The Atheroprotective Activities Mediated by SR-BI in Liver and Peripheral Tissues Are Conserved under CETP Expressing Conditions—We previously clearly evidenced a SR-BI dose-dependent effect on the development of atherosclerosis when comparing WT, hypomSR-BI, hypomSR-BI KO^{liver}, and SR-BI$^{-/-}$ mice fed an inflammatory and atherogenic (cholesterol and cholate-containing) diet (4). The impact of CETP expression on atherogenesis in these various mouse lines was evaluated by feeding female mice a 1.25C diet for 20 weeks. This diet resulted in a moderate elevation of plasma TC as compared with chow-fed conditions (Tables 1 and 2), but more cholesterol was found associated with VLDL-sized lipoproteins in all models (Fig. 6, *A* and *B*). Expression of CETP in WT background was pro-atherogenic as previously reported (34) and resulted in a 1.7-fold increase in mean lipid lesion area (Fig. 6*C*). Knock-down expression of SR-BI in hypomSR-BI mice is equally pro-atherogenic (4) and led to a similar increase in atherosclerosis as compared with WT. Interestingly, the size of lipid lesions in hypomSR-BI and hypomSR-BI/CETP mice were not different ($71 \pm 14 \times 10^3$ μm^2 and $72 \pm 26 \times 10^3$ μm^2, respectively), despite reduced plasma TC levels in CETP-expressing mice (Table 2). However, whereas CETP activity tended to increase HDL-C levels in normal-sized HDL particles (large HDL were not detectable in hypomSR-BI/CETP mice), it also led to a major increase in VLDL-C, suggesting dual pro- and anti-atherogenic actions of CETP in hypomSR-BI mice with a neutral effect on atherosclerosis susceptibility. Fed the 1.25C diet, SR-BI liver-deficient and fully deficient mice had a further increase in their plasma FC:TC ratio, which reached a value of 0.62 ± 0.03 for both models (Table 2). Deletion of hepatic SR-BI was highly atherogenic and a further 4.1-fold increase in the size of lipid lesions ($295 \pm 53 \times 10^3$ μm^2) was observed in hypomSR-BI KO^{liver} mice as compared with hypomSR-BI mice (Fig. 6*C*). Despite similar lipoprotein cholesterol profiles (Fig. 6*B*), plasma TC and FC:TC levels (Table 2), SR-BI$^{-/-}$ mice exhibited an even greater susceptibility to atherosclerotic lesion development as compared with hypomSR-BI KO^{liver} animals ($p < 0.05$). These data further support the conclusions of our previous study of a peripheral atheroprotective role mediated by SR-BI (4). In these SR-BI-

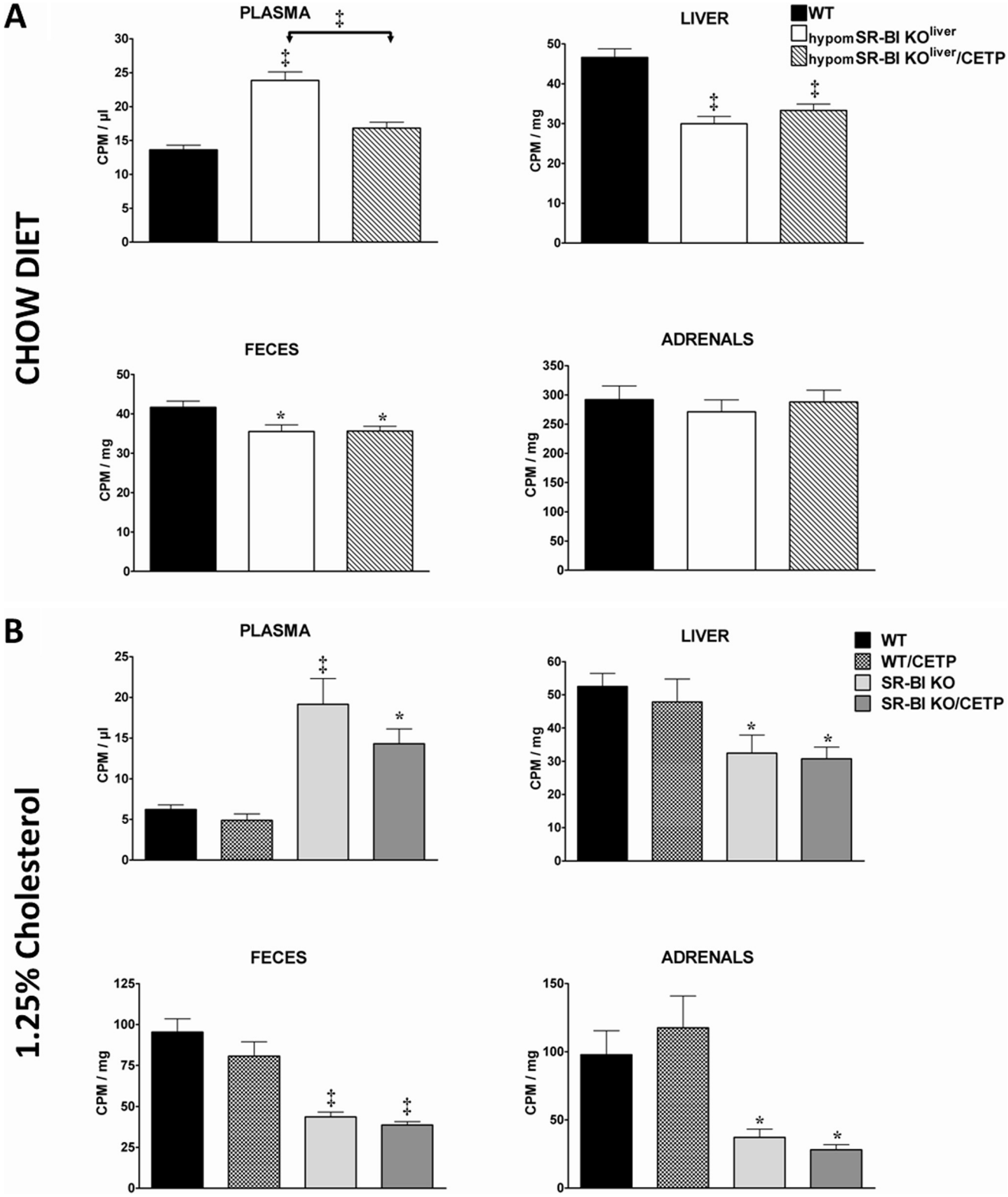

FIGURE 5. ***In vivo* macrophage to feces RCT studies.** Mice were injected intraperitoneally with [^{3}H]cholesterol-labeled BM-derived macrophages and the amount of radioactivity present in plasma, liver, feces, and adrenals was determined 48 h later. RCT experiments were performed in 3–4-month-old (*A*) female mice ($n = 7$) fed a chow diet and (*B*) male mice ($n = 6$) fed a 1.25C diet (1.25% cholesterol, 20% fat) for 4 weeks. Data represent mean ± S.E. *, $p < 0.05$; †, $p < 0.01$; ‡, $p < 0.001$.

deficient mouse models, CETP expression markedly lowered plasma TC levels (Table 2) by primarily reducing the amount of cholesterol present in large HDL particles, albeit without fully normalizing the HDL-C profile in both mouse models. VLDL-C appeared also slightly diminished in CETP-expressing mice as compared with non-CETP transgenics (Fig. 6*B*). These changes were associated with a marked reduction in atherosclerosis susceptibility in both hypomSR-BI KO^{liver}/CETP and SR-

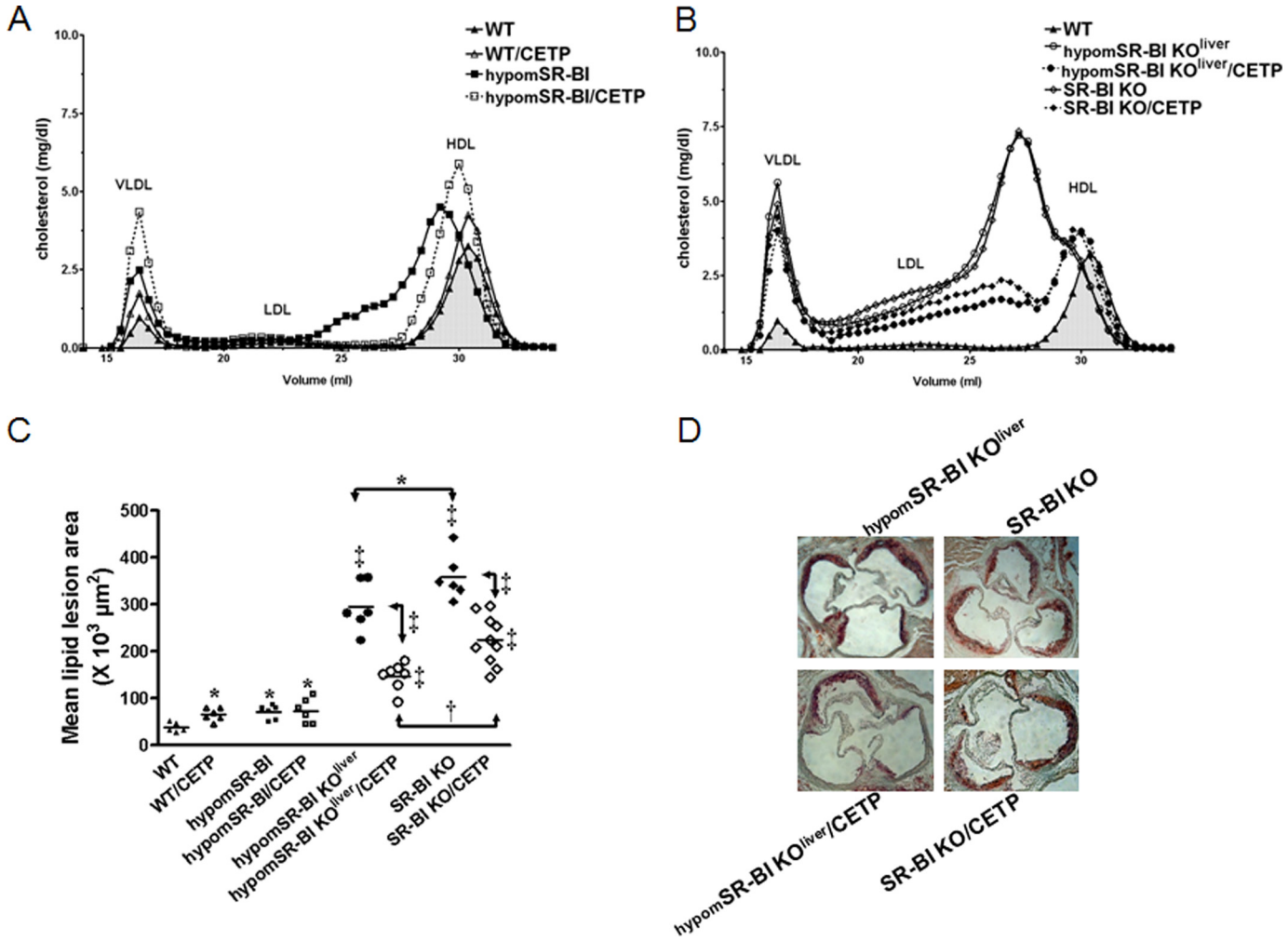

FIGURE 6. **Evaluation of the atheroprotective activities mediated by SR-BI in liver and peripheral tissues in mice expressing CETP or not and fed an atherogenic 1.25C diet.** *A* and *B*, plasma lipoprotein cholesterol profiles of female mice fed the 1.25C diet for 20 weeks. *C*, degree of atherosclerosis in the aortic root area. Lipid deposits were visualized by ORO staining of aortic root sections. Each symbol represents the mean lesion area in a single mouse. The *horizontal bar* indicates the mean value for the respective group. *, †, and ‡ denote a statistical difference *versus* WT mice or between indicated groups, *, $p < 0.05$; †, $p < 0.01$; ‡, $p < 0.001$. *D*, representative images of ORO staining of aortic root sections.

BI$^{-/-}$/CETP mice as compared with hypomSR-BI KO^{liver} ($p < 0.001$) and SR-BI$^{-/-}$ ($p < 0.001$) mice, respectively (Fig. 6, *C* and *D*). Interestingly and as observed for non-CETP transgenic models, hypomSR-BI KO^{liver}/CETP exhibited less aortic lipid lesions than SR-BI$^{-/-}$/CETP mice (1.5-fold, $p < 0.01$) at comparable plasma cholesterol distribution (Fig. 6*C*) and levels (Table 2).

DISCUSSION

In this study, we have shown that CETP expression in mice almost fully masked any variations in SR-BI expression and its consequences on modulating plasma HDL-C levels (and HDL particle size), most likely by promoting plasma HDL-C clearance. However, our data also highlighted that CETP expression could not compensate for the lack of SR-BI in adrenal glands to ensure cholesterol supply and normal function, and in hepatocytes to regulate the amount of plasma free cholesterol, and as a consequence erythrocyte cholesterol content, and to promote macrophage to feces RCT. These hepatic SR-BI activities most likely contributed to the major atheroprotective role of SR-BI. Importantly, we demonstrated that in a similar lipoprotein context and in the presence or absence of the CETP pathway, residual peripheral SR-BI expression contributed to significant atheroprotection.

Complete deletion of SR-BI in mice has been associated with an impaired RCT, whereas overexpression of SR-BI in the liver promoted macrophage RCT (8). We confirmed that SR-BI$^{-/-}$ mice exhibited a decreased rate of cholesterol transport from plasma HDL and macrophages but, we also demonstrated that deletion of SR-BI in the liver led to similar results. These new findings strongly suggest that hepatic SR-BI expression directly regulates the rate of RCT, most probably through hepatic uptake of HDL-C. However, an indirect role of hepatic SR-BI in modulating the capacity of HDL particle to mobilize cholesterol from macrophages due to changes in their composition/structure cannot be fully excluded. In fact, if the large CE-rich HDL particles present in hypomSR-BI KO^{liver} mice almost disappeared in CETP transgenic mice, the plasma FC:TC ratio remained elevated; a condition that may not favor peripheral cellular cholesterol efflux. Our results also support the notion that the RCT rate cannot be predicted as a function of the steady-state plasma concentration of HDL-C/APOA-I.

CETP-mediated transfer of CE from HDL to VLDL/LDL particles with subsequent uptake primarily by hepatic LDL-r constitutes a major quantitative route for delivery of cholesterol to the liver in humans. The capacity of CETP to significantly accelerate RCT from plasma HDL in liver-deficient mice clearly demonstrated that this pathway does not rely on a functional hepatic SR-BI receptor. However, animal studies that have been undertaken to demonstrate a direct contribution of CETP in accelerating macrophage to feces RCT have led to contradictory results (14–18). Studies that reported a role of CETP in RCT have used either [^{3}H]cholesterol-labeled RAW264.7 or J774 cells in their *in vivo* RCT assay (14, 15). These macrophage cell lines do not produce APOE (35). Yet, this apolipoprotein is very abundantly secreted from macrophages (35, 36) and macrophage-derived APOE plays a critical role in promoting macrophage-RCT (37). Whether the lack of effect of CETP on the RCT rate in our studies could be due to the fact that [^{3}H]cholesterol originating from macrophages essentially through an endogenous APOE-dependent efflux pathway is primarily directed to the liver in an APOE-dependent manner for excretion remains an intriguing possibility. In RCT studies performed with macrophage cell lines that do not express APOE, [^{3}H]cholesterol efflux from macrophage could rely more on exogenous HDL/APOA-I acceptors and may be more directly subjected to CETP-mediated transfer to VLDL/LDL for subsequent liver uptake, allowing demonstration of a role of CETP in promoting RCT under these experimental conditions.

Circulating HDL is a major source of cholesterol for steroid synthesis in mice and SR-BI is uniquely responsible for the selective uptake of HDL-CE in this organ (9). Decreased adrenal steroidogenesis in members of a family heterozygous for a functional mutation (P297S) in the *SCARB1* gene suggests that the HDL/SR-BI tandem also plays a critical function in regulating adrenal function in humans (38). In this study, moderate and severe adrenal cholesterol depletion in hypomSR-BI mice, which exhibit reduced SR-BI expression, and SR-BI$^{-/-}$ mice, respectively, further support the key contribution of SR-BI to adrenal cholesterol supply. However, it is striking that hypomSR-BI KO^{liver} mice expressing CETP or not accumulated cholesterol in their adrenal glands, whereas they also displayed attenuated adrenal SR-BI expression. As suggested above, a high plasma FC:TC ratio in these mice may alter the bidirectional cholesterol movement between adrenal cortical cell membranes and extracellular cholesterol acceptors; limiting cellular cholesterol efflux and/or favoring SR-BI-mediated cholesterol influx. Additional studies are required to investigate these potential mechanisms. Nevertheless, our results further highlight the key role of SR-BI in RCT and emphasize the fact that suppression of the hepatic step of this pathway may affect cellular cholesterol homeostasis in peripheral tissues, even when CETP is present.

In the recent report of Vergeer *et al.* (38), heterozygous carriers of the P297S SR-BI mutation, who displayed increased HDL cholesterol levels, did not seem to develop more atherosclerosis than family noncarriers (38). In this regard, it is interesting to note that if knockdown expression of SR-BI has been systematically associated with increased atherogenesis in mice (4, 5, 39), reduced levels of SR-BI in mice expressing CETP was not pro-atherogenic despite an elevation of plasma TC (hypomSR-BI/CETP *versus* WT/CETP; Table 2). These results suggest that remodeling of HDL particles by CETP, despite being associated with an increase in circulating levels of VLDL-C (Fig. 6), may counterbalance the pro-atherogenic consequences of the attenuated levels of SR-BI. By contrast, in the context of a complete absence of hepatic SR-BI, and thus of impaired RCT, CETP activity conferred only partial atheroprotection. Most importantly, additional deletion of residual SR-BI expression in extrahepatic tissues favored atherosclerosis development in a comparable manner whether CETP was present or not. Thus, using different atherogenic diets (1.25% cholesterol-enriched diets containing cholate (4) or not (this study)) and in different contexts of cholesterol transport (presence or absence of CETP), we clearly demonstrated the peripheral atheroprotective role mediated by SR-BI. Whether such a protective role relies on the multiligands receptor nature of SR-BI, its function in steroidogenic tissues for cholesterol supply, its activities in promoting endothelial repair (40), in facilitating endothelial nitric oxide (NO) production (41), or inversely in protecting against NO cytotoxicity (42), or as a modulator of the inflammatory response in macrophages (43) remains to be established. Cross-breeding of the hypomSR-BI mouse model with cell-specific CRE transgenic lines should provide valuable mouse models to investigate these possibilities.

In conclusion, on the foreground of these studies it can be postulated that SR-BI plays a critical function in the liver in regulating the flux of circulating free cholesterol and acts as an anti-atherogenic molecule, potentially in various tissues, in species that express CETP or not. However, it can also be foreseen that variations in hepatic SR-BI activity shall not translate into major changes in the plasma concentrations of cholesterol in CETP-expressing species, and notably in humans. In this context and in the framework of the actual development of CETP inhibitors as pharmacological lipid-modulating agents, the potential use of such agents in individuals with homozygous loss-of-function mutations in the *SCARB1* gene could favor a highly atherogenic situation.

REFERENCES

1. Kozarsky, K. F., Donahee, M. H., Rigotti, A., Iqbal, S. N., Edelman, E. R., and Krieger, M. (1997) *Nature* **387,** 414–417
2. Ueda, Y., Gong, E., Royer, L., Cooper, P. N., Francone, O. L., and Rubin, E. M. (2000) *J. Biol. Chem.* **275,** 20368–20373
3. Ueda, Y., Royer, L., Gong, E., Zhang, J., Cooper, P. N., Francone, O., and Rubin, E. M. (1999) *J. Biol. Chem.* **274,** 7165–7171
4. Huby, T., Doucet, C., Dachet, C., Ouzilleau, B., Ueda, Y., Afzal, V., Rubin, E., Chapman, M. J., and Lesnik, P. (2006) *J. Clin. Invest.* **116,** 2767–2776
5. Huszar, D., Varban, M. L., Rinninger, F., Feeley, R., Arai, T., Fairchild-Huntress, V., Donovan, M. J., and Tall, A. R. (2000) *Arterioscler. Thromb. Vasc. Biol.* **20,** 1068–1073
6. Rigotti, A., Trigatti, B. L., Penman, M., Rayburn, H., Herz, J., and Krieger, M. (1997) *Proc. Natl. Acad. Sci. U.S.A.* **94,** 12610–12615
7. Van Eck, M., Twisk, J., Hoekstra, M., Van Rij, B. T., Van der Lans, C. A., Bos, I. S., Kruijt, J. K., Kuipers, F., and Van Berkel, T. J. (2003) *J. Biol. Chem.* **278,** 23699–23705
8. Zhang, Y., Da Silva, J. R., Reilly, M., Billheimer, J. T., Rothblat, G. H., and Rader, D. J. (2005) *J. Clin. Invest.* **115,** 2870–2874
9. Out, R., Hoekstra, M., Spijkers, J. A., Kruijt, J. K., van Eck, M., Bos, I. S., Twisk, J., and Van Berkel, T. J. (2004) *J. Lipid Res.* **45,** 2088–2095

10. Wang, X., Collins, H. L., Ranalletta, M., Fuki, I. V., Billheimer, J. T., Rothblat, G. H., Tall, A. R., and Rader, D. J. (2007) *J. Clin. Invest.* **117,** 2216–2224
11. Gauthier, A., Lau, P., Zha, X., Milne, R., and McPherson, R. (2005) *Arterioscler. Thromb. Vasc. Biol.* **25,** 2177–2184
12. Zhou, H., Li, Z., Silver, D. L., and Jiang, X. C. (2006) *Biochim. Biophys. Acta* **1761,** 1482–1488
13. Schwartz, C. C., VandenBroek, J. M., and Cooper, P. S. (2004) *J. Lipid Res.* **45,** 1594–1607
14. Tchoua, U., D'Souza, W., Mukhamedova, N., Blum, D., Niesor, E., Mizrahi, J., Maugeais, C., and Sviridov, D. (2008) *Cardiovasc. Res.* **77,** 732–739
15. Tanigawa, H., Billheimer, J. T., Tohyama, J., Zhang, Y., Rothblat, G., and Rader, D. J. (2007) *Circulation* **116,** 1267–1273
16. Rotllan, N., Calpe-Berdiel, L., Guillaumet-Adkins, A., Süren-Castillo, S., Blanco-Vaca, F., and Escolà-Gil, J. C. (2008) *Atherosclerosis* **196,** 505–513
17. Harada, L. M., Amigo, L., Cazita, P. M., Salerno, A. G., Rigotti, A. A., Quintão, E. C., and Oliveira, H. C. (2007) *Atherosclerosis* **191,** 313–318
18. Stein, O., Dabach, Y., Hollander, G., Ben-Naim, M., Halperin, G., and Stein, Y. (2002) *Atherosclerosis* **164,** 73–78
19. Brousseau, M. E., Diffenderfer, M. R., Millar, J. S., Nartsupha, C., Asztalos, B. F., Welty, F. K., Wolfe, M. L., Rudling, M., Björkhem, I., Angelin, B., Mancuso, J. P., Digenio, A. G., Rader, D. J., and Schaefer, E. J. (2005) *Arterioscler. Thromb. Vasc. Biol.* **25,** 1057–1064
20. Postic, C., and Magnuson, M. A. (2000) *Genesis* **26,** 149–150
21. Lesnik, P., Haskell, C. A., and Charo, I. F. (2003) *J. Clin. Invest.* **111,** 333–340
22. Zhang, Y., Zanotti, I., Reilly, M. P., Glick, J. M., Rothblat, G. H., and Rader, D. J. (2003) *Circulation* **108,** 661–663
23. Harder, C., Lau, P., Meng, A., Whitman, S. C., and McPherson, R. (2007) *Arterioscler. Thromb. Vasc. Biol.* **27,** 858–864
24. Hildebrand, R. B., Lammers, B., Meurs, I., Korporaal, S. J., De Haan, W., Zhao, Y., Kruijt, J. K., Praticò, D., Schimmel, A. W., Holleboom, A. G., Hoekstra, M., Kuivenhoven, J. A., Van Berkel, T. J., Rensen, P. C., and Van Eck, M. (2010) *Arterioscler. Thromb. Vasc. Biol.* **30,** 1439–1445
25. Braun, A., Zhang, S., Miettinen, H. E., Ebrahim, S., Holm, T. M., Vasile, E., Post, M. J., Yoerger, D. M., Picard, M. H., Krieger, J. L., Andrews, N. C., Simons, M., and Krieger, M. (2003) *Proc. Natl. Acad. Sci. U.S.A.* **100,** 7283–7288
26. Lee, J. Y., Badeau, R. M., Mulya, A., Boudyguina, E., Gebre, A. K., Smith, T. L., and Parks, J. S. (2007) *J. Lipid Res.* **48,** 1052–1061
27. Ma, K., Forte, T., Otvos, J. D., and Chan, L. (2005) *Arterioscler. Thromb. Vasc. Biol.* **25,** 149–154
28. Ji, Y., Wang, N., Ramakrishnan, R., Sehayek, E., Huszar, D., Breslow, J. L., and Tall, A. R. (1999) *J. Biol. Chem.* **274,** 33398–33402
29. Meurs, I., Hoekstra, M., van Wanrooij, E. J., Hildebrand, R. B., Kuiper, J., Kuipers, F., Hardeman, M. R., Van Berkel, T. J., and Van Eck, M. (2005) *Exp. Hematol.* **33,** 1309–1319
30. Holm, T. M., Braun, A., Trigatti, B. L., Brugnara, C., Sakamoto, M., Krieger, M., and Andrews, N. C. (2002) *Blood* **99,** 1817–1824
31. Dole, V. S., Matuskova, J., Vasile, E., Yesilaltay, A., Bergmeier, W., Bernimoulin, M., Wagner, D. D., and Krieger, M. (2008) *Arterioscler. Thromb. Vasc. Biol.* **28,** 1111–1116
32. Hoekstra, M., Ye, D., Hildebrand, R. B., Zhao, Y., Lammers, B., Stitzinger, M., Kuiper, J., Van Berkel, T. J., and Van Eck, M. (2009) *J. Lipid Res.* **50,** 1039–1046
33. Sehayek, E., and Hazen, S. L. (2008) *Arterioscler. Thromb. Vasc. Biol.* **28,** 1296–1297
34. Marotti, K. R., Castle, C. K., Boyle, T. P., Lin, A. H., Murray, R. W., and Melchior, G. W. (1993) *Nature* **364,** 73–75
35. Werb, Z., and Chin, J. R. (1983) *J. Cell Biol.* **97,** 1113–1118
36. Kockx, M., Guo, D. L., Huby, T., Lesnik, P., Kay, J., Sabaretnam, T., Jary, E., Hill, M., Gaus, K., Chapman, J., Stow, J. L., Jessup, W., and Kritharides, L. (2007) *Circ. Res.* **101,** 607–616
37. Zanotti, I., Pedrelli, M., Potì, F., Stomeo, G., Gomaraschi, M., Calabresi, L., and Bernini, F. (2011) *Arterioscler. Thromb. Vasc. Biol.* **31,** 74–80
38. Vergeer, M., Korporaal, S. J., Franssen, R., Meurs, I., Out, R., Hovingh, G. K., Hoekstra, M., Sierts, J. A., Dallinga-Thie, G. M., Motazacker, M. M., Holleboom, A. G., Van Berkel, T. J., Kastelein, J. J., Van Eck, M., and Kuivenhoven, J. A. (2011) *N. Engl. J. Med.* **364,** 136–145
39. Kocher, O., Yesilaltay, A., Shen, C. H., Zhang, S., Daniels, K., Pal, R., Chen, J., and Krieger, M. (2008) *Biochim. Biophys. Acta* **1782,** 310–316
40. Seetharam, D., Mineo, C., Gormley, A. K., Gibson, L. L., Vongpatanasin, W., Chambliss, K. L., Hahner, L. D., Cummings, M. L., Kitchens, R. L., Marcel, Y. L., Rader, D. J., and Shaul, P. W. (2006) *Circ. Res.* **98,** 63–72
41. Yuhanna, I. S., Zhu, Y., Cox, B. E., Hahner, L. D., Osborne-Lawrence, S., Lu, P., Marcel, Y. L., Anderson, R. G., Mendelsohn, M. E., Hobbs, H. H., and Shaul, P. W. (2001) *Nat. Med.* **7,** 853–857
42. Li, X. A., Guo, L., Asmis, R., Nikolova-Karakashian, M., and Smart, E. J. (2006) *Circ. Res.* **98,** e60–65
43. Guo, L., Song, Z., Li, M., Wu, Q., Wang, D., Feng, H., Bernard, P., Daugherty, A., Huang, B., and Li, X. A. (2009) *J. Biol. Chem.* **284,** 19826–19834